Large Scale Profiling of Phospho-proteins in Cell and Tissue Microarrays using Phospho-Specific Antibodies: Identification of Biomarkers and Pharmacodynamic activity for a c-Kit inhibitor.

Herbert Haack, Laura C. Sullivan, Andrew Garton, John D. Haley, Bradley L. Smith. • Cell Signaling Technology, Danvers, MA • OSI Pharmaceuticals Inc., Farmingdale, NY

Introduction

Achieving cellular resolution in the analysis of proteomic patterns would greatly benefit our understanding of the efficacy and mechanism of action of therapeutic agents. We have used model cell lines and xenografts in large-scale tissue microarray screens with phospho-specific antibodies to identify potential biomarkers for the inhibitor OSI-930, a small molecule inhibitor of kit and KDR kinases. The inhibitor has shown growth inhibitory and pro-apoptotic effects in mast cell and SCLC lines *in vitro* and shows tumor growth inhibitory activity in corresponding xenograft models *in vivo*. Five cell and six xenograft models were exposed to the compound and then fixed, embedded and arrayed for IHC analysis. Over 150 phospho-specific and total antibodies, containing components of many of the known signaling pathways were used for expression profiling. The antibodies were systematically validated for IHC before use on the test samples. A total of 4 arrays containing different time points and drug concentrations were analyzed and over 30,000 array-cores were subjectively scored.

Methods

Xenografts were initiated using 5-10x10^6 cells in 50% Matrigel™ injected subcutaneously into NCR/nu mice. Upon harvest tumors were divided into multiple pieces. Tissues were either snap frozen in liquid nitrogen and embedded in OCT or fixed for 24 hours in 10% neutral buffered formalin, then processed and embedded in paraffin per standard methods. Frozen sections were cut at 7-8 µm and paraffin sections were cut at 4-5 µm. Immunohistochemical analysis on frozen and paraffin sections was performed according to standard CST protocols, with primary antibody incubations overnight at 4°C using the same recommended dilution for frozen and paraffin staining. All antibodies were from CST.

Summary of the pharmacodynamic effects of OSI-930.

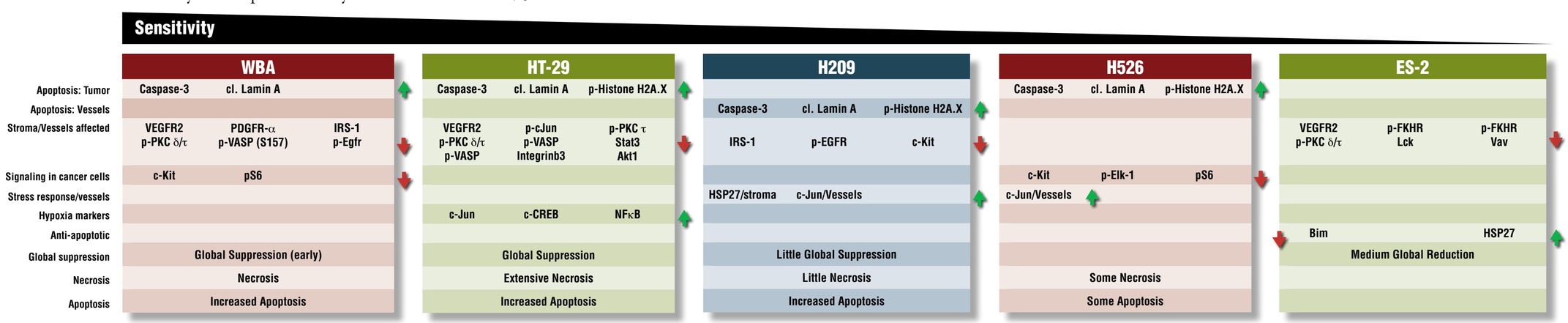

Project outline.

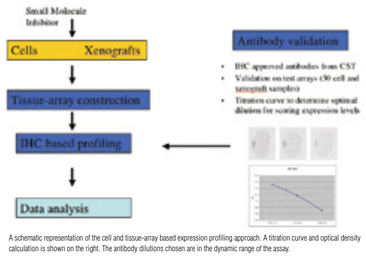

A schematic representation of the cell and tissue-array based expression profiling approach. A titration curve and optical density calculation is shown on the right. The antibody dilutions chosen are in the dynamic range of the assay.

Target effects.

	HT-29	H526	ES-2	WBA	H209	HCT116
c-Kit	0	3	0	2	1	0
VEGFR2	2 vessels / 2 cancer	2 vessels / 1 cancer	2 vessels / 1 cancer	2 vessels / 1 cancer	2 vessels / 1 cancer	2 vessels / 1 cancer
PDGFR β	3 stroma	2 stroma	3 stroma	3 stroma	1 stroma	2 stroma
PDGFR α	1 stroma	3 stroma	3 stroma	3 stroma	3 stroma	2 stroma

Table (above) summarizing the expression level in xenografts of four major targets that are inhibited by OSI-930. As an example, staining with a c-Kit antibody is shown in the images (left) for xenografts HT-29 (no expression = 0) and H526 (high expression = 3). Legend describes the color coding for the four expression levels (0-4).

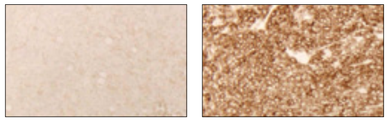

Xenograft growth response.

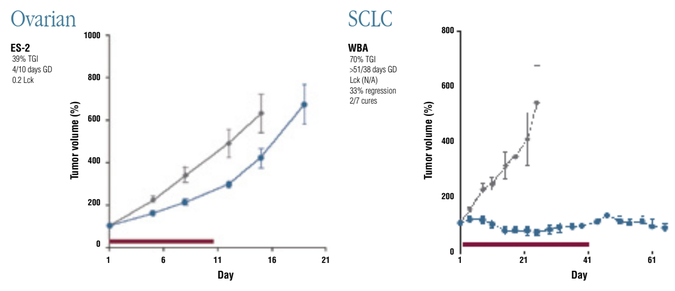

Mediators of angiogenesis.

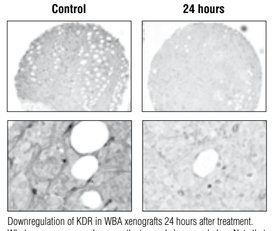

Downregulation of KDR in WBA xenografts 24 hours after treatment. Whole array cores are shown on the top and close-ups below. Note that staining is strongly reduced in both vessels and tumor cells.

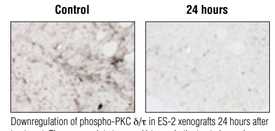

Downregulation of phospho-PKC δ/τ in ES-2 xenografts 24 hours after treatment. The arrow points to vessel/stroma in the treated sample.

Loss of KDR within 24 hours of drug treatment.

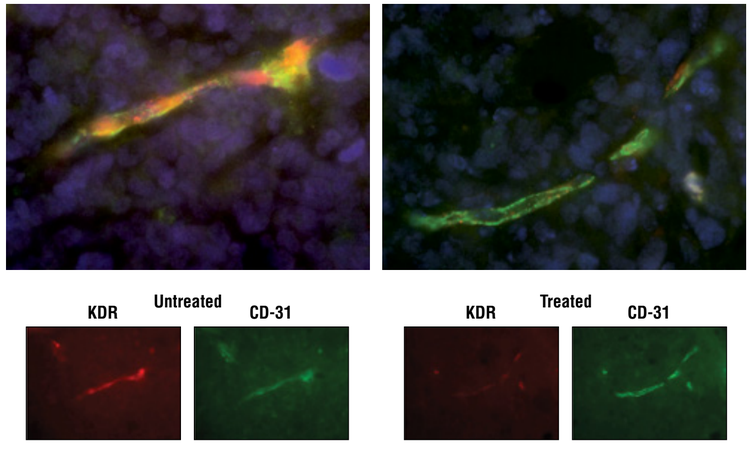

Summary

The screening of xenografts and embedded cell pellets (results not shown) allowed us to compile a response profile for OSI-930 and lead to the identification of about 30 targets that are altered in cells or tumors in response to the inhibitor. Specific tumor and stromal activities of compound OSI-930 were identified in xenograft arrays. The changes closely reflect the compounds effect on xenograft growth inhibition, and increases in apoptosis and necrosis. For example, effects on signaling in tumor cells (p-S6 ribosomal protein) was only seen in the two xenograft models that express the receptor tyrosine kinase c-kit. All tumors treated with compound OSI–930 showed reduction in a number of stromal/blood vessel markers, and interestingly downstream components of VEGFR-2 signaling (p-PKC, p-Erk). In contrast, in the non-responding xenograft model (ES-2), a downregulation of vessel markers was observed but no change in apoptosis markers occurred. Instead, changes in HSP-27 and Bim, a pro-apoptotic protein, occurred in response to the inhibitor that might contribute to the resistance of the ES-2 xenografts. None of the changes discussed were observed in the HCT-116 xenografts that were treated with an unrelated compound.

The markers that were identified in this screen closely reflect the underlying biology of the major targets of OSI-930 and give us a better understanding of the drug's modes of action.

Acknowledgements

We thank Shannon Winski, Mary Srebernak and Gina Sennello for generating and preparing the xenografts and Dr. Joseph Butterfield and Dr. Geoffrey Krystal for providing HMC-1 and WBA cells, respectively.

Cell Signaling TECHNOLOGY®

www.cellsignal.com